Reassessment of the Burns temperature and its relationship to the diffuse scattering, lattice dynamics, and thermal expansion in relaxor $Pb(Mg_{1/3}Nb_{2/3})O_3$

P. M. Gehring,[1] H. Hiraka,[2,3] C. Stock,[4] S.-H. Lee,[1] W. Chen,[5] Z.-G. Ye,[5] S. B. Vakhrushev,[6] and Z. Chowdhuri[1]
[1]*NIST Center for Neutron Research, National Institute of Standards and Technology, Gaithersburg, Maryland 20899-6100, USA*
[2]*Department of Physics, Brookhaven National Laboratory, Upton, New York 11973-5000, USA*
[3]*Institute for Materials Research, Tohoku University, Sendai 980-8577, Japan*
[4]*ISIS Facility, Rutherford Appleton Laboratory, Chilton, Didcot OX11 0QX, United Kingdom*
[5]*Department of Chemistry, Simon Fraser University, Burnaby, British Columbia, Canada V5A 1S6*
[6]*Ioffe Physical-Technical Institute, 26 Politekhnicheskaya, 194021 St. Petersburg, Russia*
(Received 27 March 2008; revised manuscript received 27 April 2009; published 9 June 2009)

We have used neutron scattering techniques that probe time scales from 10^{-12} to 10^{-9} s to characterize the diffuse scattering and low-energy lattice dynamics in single crystals of the relaxor $PbMg_{1/3}Nb_{2/3}O_3$ (PMN) from 10 to 900 K. Our study extends far below $T_c=213$ K, where long-range ferroelectric correlations have been reported under field-cooled conditions, and well above the nominal Burns temperature $T_d\approx 620$ K, where optical measurements suggest the development of short-range polar correlations known as "polar nanoregions" (PNR). We observed two distinct types of diffuse scattering. The first is weak, relatively temperature independent, persists to at least 900 K, and forms bow-tie-shaped patterns in reciprocal space centered on (h00) Bragg peaks. We associate this primarily with chemical short-range order. The second is strong, temperature dependent, and forms butterfly-shaped patterns centered on (h00) Bragg peaks. This diffuse scattering has been attributed to the PNR because it responds to an electric field and vanishes near $T_d\approx 620$ K when measured with thermal neutrons. Surprisingly, it vanishes at 420 K when measured with cold neutrons, which provide approximately four times superior energy resolution. That this onset temperature depends so strongly on the instrumental energy resolution indicates that the diffuse scattering has a quasielastic character and demands a reassessment of the Burns temperature T_d. Neutron backscattering measurements made with 300 times better energy resolution confirm the onset temperature of 420 ± 20 K. The energy width of the diffuse scattering is resolution limited, indicating that the PNR are static on time scales of at least 2 ns between 420 and 10 K. Transverse acoustic (TA) phonon lifetimes, which are known to decrease dramatically for wave vectors $q\approx 0.2$ Å^{-1} and $T_c<T<T_d$, are temperature independent up to 900 K for q close to the zone center. This motivates a physical picture in which sufficiently long-wavelength TA phonons average over the PNR; only those TA phonons having wavelengths comparable to the size of the PNR are affected. Finally, the PMN lattice constant changes by less than 0.001 Å below 300 K but expands rapidly at a rate of 2.5×10^{-5} K^{-1} at high temperature. These disparate regimes of low and high thermal expansions bracket the revised value of T_d, which suggests the anomalous thermal expansion results from the condensation of static PNR.

DOI: 10.1103/PhysRevB.79.224109 PACS number(s): 77.84.Dy, 77.65.−j, 77.80.Bh

I. INTRODUCTION

The concept of nanometer-scale regions of polarization, randomly embedded within a nonpolar cubic matrix, has become central to attempts to explain the remarkable physical properties of relaxors such as $PbMg_{1/3}Nb_{2/3}O_3$ (PMN) and $PbZn_{1/3}Nb_{2/3}O_3$ (PZN).[1–4] The existence of these so-called "polar nanoregions" (PNR) was first inferred from the optic index of refraction studies of Burns and Dacol[5] on PMN, PZN, and other related systems and later confirmed using many different experimental techniques including x-ray and neutron diffraction,[6–9] ^{207}Pb NMR,[10] and piezoresponse force microscopy.[11] Early small-angle x-ray scattering and neutron pair distribution function (PDF) measurements on PMN by Egami *et al.*[12] cast doubt on the nanodomain model of relaxors. However, the recent PDF analysis of Jeong *et al.*,[13] which shows the formation of polar ionic shifts in PMN below ≈650 K and which occupies only one third of the total sample volume at low temperatures, provides convincing support for the existence of PNR. Neutron inelastic scattering data published by Naberezhnov *et al.*[14] on PMN offered the first dynamical evidence of PNR in the form of a prominent broadening of the transverse acoustic (TA) mode that coincides with the onset of strong diffuse scattering at 650 K,[15] roughly the same temperature (≈620 K) as that reported by Burns and Dacol[5] in their optical study of PMN. This temperature, commonly known as the Burns temperature, and denoted by T_d in the original paper, is widely viewed as that at which static PNR first appear. Likely condensing from a soft transverse optic (TO) mode, distinctive butterfly-shaped and ellipsoidal diffuse scattering intensity contours centered on (h00) and (hh0) Bragg peaks, respectively, are seen below T_d in both PMN (Refs. 16–18) and PZN.[19] Similar diffuse scattering patterns were subsequently observed in solid solutions of PMN and PZN with $PbTiO_3$ (PMN-xPT and PZN-xPT); however these patterns appear only on the Ti-poor (relaxor) side of the well-known morphotropic phase boundary (MPB).[20,21] The polar nature of the strong diffuse scattering, and thus its association with the formation of PNR, was unambiguously established by several electric field studies of PMN (Refs. 22 and 23) and PZN-8%PT,[19,24–26] all of which showed dramatic changes in

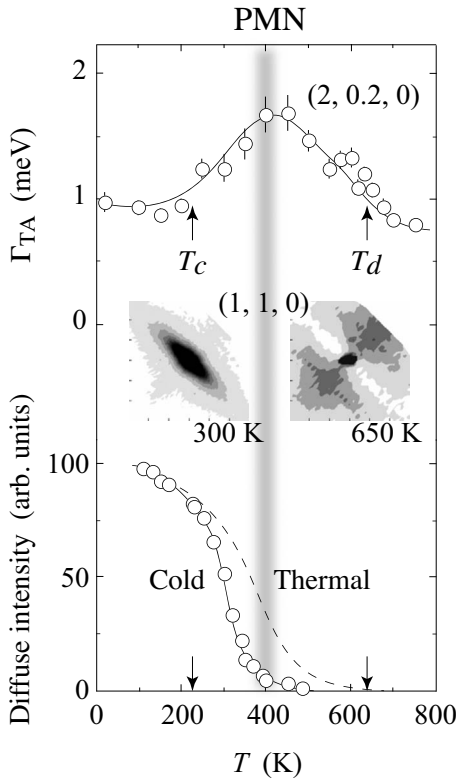

FIG. 1. Top—temperature dependence of the TA phonon energy width Γ_{TA} measured with thermal neutrons by Wakimoto *et al.* (Ref. 27). Middle—diffuse scattering intensity contours measured at (110) below (300 K) and just above (650 K) the Burns temperature T_d using cold neutrons by Hiraka *et al.* (Ref. 28). Bottom-diffuse scattering temperature dependence measured with cold neutrons (open circles) and thermal neutrons (dashed line) by Hiraka *et al.* (Ref. 28).

the shape and intensity of the diffuse scattering as a function of field strength and field orientation. The Burns temperature T_d thus represents what is arguably the most important temperature scale in relaxors and is several hundred degrees kelvin higher than the critical temperature T_c (which for PMN is $\approx$210 K but defined only in nonzero electric field).

Recent studies of the neutron diffuse scattering in PMN by Stock *et al.*[29] and especially those by Hlinka *et al.*[30] and Gvasaliya *et al.*[31,32] have proven to be extremely important because they demonstrated the utility of cold neutron spectroscopy to the study of relaxors. Generally speaking cold neutrons are ill-suited to lattice dynamical studies because the longer wavelengths necessarily limit their use to the study of comparatively fewer (lower-Q) Brillouin zones. On the other hand cold neutron spectrometers provide significantly better energy ($\hbar\omega$) and wave vector (q) resolution than do their thermal neutron counterparts. In addition, both the (110) and the (100) Brillouin zones of PMN are accessible using cold neutrons with wavelengths $\lambda \approx 4.26$ Å. The combined cold and thermal neutron study of PMN by Hiraka *et al.*[28] exploited this fact and uncovered several major findings, two of which are summarized in Fig. 1. The first finding is that the temperature at which the strong diffuse scattering vanishes depends on whether the measurement is made with cold or thermal neutrons, i.e., the value of T_d depends on the energy resolution of the spectrometer. This fact, which is illustrated in the bottom panel of Fig. 1, indicates that the diffuse scattering in PMN, and most likely other relaxors, contains a substantial quasielastic component. However, a consensus on this issue is lacking; while the finding of Hiraka *et al.*[28] is consistent with the study of Gvasaliya *et al.*,[31,32] it contradicts that of Hlinka *et al.*[30,33] A second major finding is displayed in the middle panel of Fig. 1 where intensity contours of the diffuse scattering measured with cold neutrons around (110) are shown to exhibit markedly different reciprocal space geometries at 300 and 650 K. These data unambiguously demonstrate the presence of two distinct types of diffuse scattering in PMN. As the PNR are absent at 650 K $\geq T_d$, the physical origin of the bow-tie-shaped diffuse scattering cross section is believed to come primarily from the underlying chemical short-range order (CSRO). We shall refer to this as CSRO, although another commonly used term for this is compositionally/chemically ordered regions (CORs).[34]

An intriguing perspective on the Burns temperature in PMN is provided in the top panel of Fig. 1 where the TA phonon energy width Γ_{TA}, which is inversely proportional to the phonon lifetime, is plotted as a function of temperature for PMN at the scattering vector $\vec{Q}=(2,0.2,0)$. These data were measured with thermal neutrons by Wakimoto *et al.*[27] and are consistent with those of Naberezhnov *et al.*[14] in that the TA mode begins to broaden at $T_d \approx 620$ K, the same temperature where the strong diffuse scattering first appears. These data also show that the TA broadening achieves a maximum value (minimum lifetime) near 420 K, which coincides with the value of T_d measured with cold neutrons. These data raise the question of how to interpret the Burns temperature T_d properly in that they paint a picture, markedly different from that currently held, in which the PNR are dynamic below $\sim$650 K and condense into static entities only at a much lower temperature of 420 K.

The goal of our study then is to determine the intrinsic value of the Burns temperature T_d and to clarify its relationship to the diffuse scattering, lattice dynamics, and structure in PMN. To this end we have carried out extensive measurements of the neutron diffuse scattering cross section from 10 to 900 K, far below T_c and well above the nominal value of T_d, which probe time scales from 10^{-12} to 10^{-9} s. We find that a 300-fold improvement in energy resolution over that used by Hiraka *et al.*,[28] obtained using neutron backscattering techniques, reproduces the same onset temperature for the diffuse scattering; hence the intrinsic Burns temperature T_d for PMN is 420 K. At the same time an enormous change in the thermal expansion is observed near 420 K, which is indistinguishable from zero at low temperature. Given the revised value of T_d, this result implies the existence of a direct influence of the PNR on the intrinsic structural properties of PMN.

We also present data on the effects of the PNR on the lattice dynamics through measurements of the temperature and wave vector dependence of the long-wavelength TA phonon energy width Γ_{TA} measured near (110) from 25 to 900 K. We find that TA modes with reduced wave vectors $q \ll 0.2$ Å^{-1} exhibit the same energy width at all temperature whereas those with $q \approx 0.2$ Å^{-1} exhibit a strongly

temperature-dependent broadening similar to that shown in the top panel of Fig. 1. This behavior contrasts with that observed in thermal neutron studies of the TO mode, which exhibits a broadening for all $q \leq 0.2$ Å^{-1}. Previous neutron scattering work on PMN-60%PT by Stock *et al.*,[35] a material in which there is no strong temperature-dependent diffuse scattering and thus no polar nanoregions, found no evidence of any TA phonon broadening. In this context, our data lend extremely strong support to the PNR model: the lifetimes of TA modes with wavelengths comparable in size to the PNR are strongly diminished by the PNR, whereas long-wavelength (low q) TA phonons simply average over the PNR and are unaffected.

II. EXPERIMENTAL DETAILS

The neutron scattering data presented here were obtained using the BT9 thermal neutron triple-axis spectrometer, the SPINS cold neutron triple-axis spectrometer, and the cold neutron high-flux backscattering spectrometer (HFBS), all of which are located at the NIST Center for Neutron Research (NCNR). On BT9, measurements of the phonons and diffuse scattering were made at a fixed final (thermal) neutron energy $E_f = 14.7$ meV ($\lambda = 2.36$ Å) using the (002) Bragg reflection of highly oriented pyrolytic graphite (HOPG) crystals to monochromate and analyze the incident and scattered neutron beams, respectively. Horizontal beam collimations were 40′-47′-S-40′-80′ (S=sample). A special nonstandard high q-resolution configuration was employed to measure the thermal expansion in which the (004) Bragg reflection from a perfect Ge crystal was used as analyzer and horizontal beam collimations were tightened to 15′-47′-S-20′-40′. The choice of Ge was motivated by the close matching between the PMN (022) (1.431 Å) and Ge (004) (1.414 Å) d spacings, which provides a significant improvement in the instrumental q resolution.[36] On SPINS, which sits on the cold neutron guide NG5, the phonon and diffuse scattering measurements were made at a fixed final neutron energy $E_f = 4.5$ meV ($\lambda = 4.264$ Å) also using the (002) Bragg reflection of HOPG crystals as monochromator and analyzer. A liquid-nitrogen cooled Be filter was located after the sample to remove higher order neutron wavelengths from the scattered beam, and horizontal beam collimations were set to guide-80′-S-80′-80′. The resultant elastic ($\hbar\omega = 0$) energy resolution for the SPINS measurements was $\delta E = 0.12$ meV half width at half maximum (HWHM).

The high-flux backscattering spectrometer was used to look for dynamics that might be associated with the strong diffuse scattering below T_d. This instrument uses a mechanically driven Si (111) monochromator to Doppler shift the energies of incident neutrons over a narrow range centered about 2.08 meV. Neutrons are backscattered from the monochromator and proceed toward the sample where they are scattered into a 12 m^2 array of Si (111) crystals that serve as analyzer. These neutrons are then backscattered a second time by the analyzer, which selects the final neutron energy $E_f = 2.08$ meV, into a series of detectors positioned about the sample. The effective angular acceptance of each detector is ≈15°. The HFBS instrument is described in further detail elsewhere.[37] The elastic energy resolution for the HFBS measurements described here was $\delta E = 0.4$ μeV (HWHM).

Two high-quality single crystals of PMN, labeled PMN 4 and PMN 5, were used in this study; both were grown using a top-seeded solution growth technique.[38] The crystal growth conditions were determined from the pseudobinary phase diagram established for PMN and PbO. The PMN 4 and 5 crystals weigh 2.7 g (0.33 cm^3) and 4.8 g (0.59 cm^3), respectively. At 300 K the mosaic of each crystal measured at (220) is less than 0.04° full width at half maximum (FWHM). Loss of PbO, the formation of a pyrochlore phase, and the reduction of Nb^{5+} are known to occur in PMN single crystals when subjected to high temperatures under vacuum for extended periods of time. This process results in a dramatic blackening of the crystal, which is normal of a transparent gold/amber color. While dielectric measurements on such darkened crystals reportedly show little difference from those on unheated samples,[39] our measurements reveal a diminishment of the diffuse scattering intensity after sustained and repeated heating. Therefore experiments on the larger PMN crystal 5 were limited to 600 K or less, while PMN crystal 4 was used to obtain data above 600 K.

Both samples were mounted with an [001] axis oriented vertically, giving access to reflections of the form ($hk0$). For the high-temperature experiments, PMN crystal 4 was wrapped in quartz wool, mounted in a niobium holder secured by tungsten wire, and then loaded into a water-cooled furnace capable of reaching temperatures from 300 to 1800 K. PMN crystal 5 was mounted onto an aluminum sample holder assembly placed inside an aluminum sample can and then loaded inside the vacuum space of a closed-cycle ^{4}He refrigerator that provides access to temperatures from 10 to 700 K. Each sample has a cubic lattice spacing of $a = 4.05$ Å at 300 K; thus 1 rlu (reciprocal lattice unit) equals $2\pi/a = 1.55$ Å^{-1}.

III. ORIGINS OF THE DIFFUSE SCATTERING: PNR VERSUS CSRO

The diffuse scattering in PMN crystal 5 was studied by Hiraka *et al.*[28] at and below the nominal Burns temperature T_d with good energy resolution ($\delta E \approx 0.12$ meV HWHM) using cold neutrons. Data were measured in the (100) and (110) Brillouin zones and are represented schematically in the upper right portion of Fig. 2. The horizontal and vertical axes in this figure correspond to the components of the scattering vector $\vec{Q} = (hk0)$, which are measured in rlu. The "low-T" ($T < T_d$) regime is dominated by contributions from the PNR, where the diffuse scattering intensity contours near (100) resemble a butterfly and those near (110) resemble an ellipse for which the long axis is oriented perpendicular to $\vec{Q}$. This is shown in Fig. 2(a) where diffuse scattering data near (100) at 300 K reveal an intense butterfly-shaped pattern.[28] We note here that we see no evidence of any "transverse component" to the diffuse scattering in any of our PMN crystals like that reported previously by Vakhrushev *et al.*[41] We assume that this component was due to the crystal imperfections mentioned by these authors in their PMN sample, which gave rise to a powder ring in their data at (100).

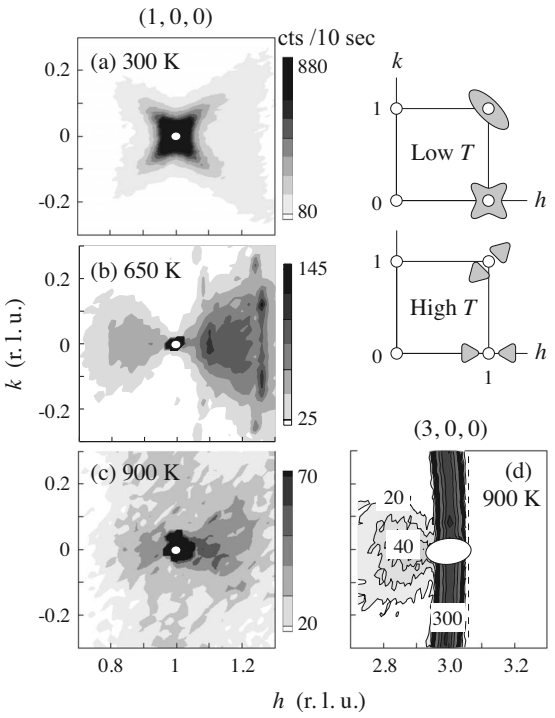

FIG. 2. Diffuse scattering intensity contours in PMN measured on SPINS near (100) are shown using a linear gray scale at (a) 300, (b) 650, and (c) 900 K. Diffuse scattering intensity contours measured on BT9 at 900 K near (300) using thermal neutrons are shown in (d). The data shown in panels (a) and (b) are from Hiraka *et al.* (Ref. 28). Schematic diagrams of the diffuse scattering intensity contours below (low-T) and at T_d (high-T) are shown in the upper right.

The same butterfly/ellipsoidal diffuse scattering geometry was shown to persist in single crystals of PMN-xPT and PZN-xPT in studies by Matsuura *et al.*[20] and Xu *et al.*,[21] respectively, for compositions spanning the Ti-poor (relaxor) side of the MPB. These results also completely refute those of La-Orauttapong *et al.*[42] who reported that the orientation of the strong diffuse scattering varies with Ti content in PZN-xPT and concluded that the PNR orientation changes with doping.[43] For Ti-rich (tetragonal) PMN-xPT compositions just beyond the MPB, Matsuura *et al.*[20] found that the strong temperature-dependent diffuse scattering vanishes and is replaced by critical scattering. Matsuura *et al.*[20] also found that the q-integrated diffuse scattering intensity increases with Ti content on the Ti-poor side of the MPB, peaks near the MPB, then drops dramatically on crossing the MPB. This finding is significant because it suggests that an intriguing and direct correlation exists between the PNR and the piezoelectric coefficient d_{33}, which exhibits the same dependence on Ti content.[2] A model based on pancake-shaped ferroelectric domains has been used successfully to fit the three-dimensional (3D) diffuse scattering distributions measured in PZN-xPT with high-energy x rays.[21,44,45] A similar type of real-space structure has been proposed to explain the diffuse scattering in the relaxor $KLi_xTa_{1-x}O_3$.[46] On the other hand, alternative models explaining the same diffuse scattering distributions have also been proposed.[47]

In the "high-T" regime ($T \geq T_d$) there are no PNR, and the associated butterfly-shaped diffuse scattering is no longer present. The weak diffuse scattering that remains is thus argued to originate primarily from the underlying CSRO, which reflects weak correlations between the Mg^{2+} and Nb^{5+} cations on the B site of the perovskite ABO_3 structure. In this regime the shapes of the diffuse scattering contours are radically different, resembling a bow-tie in both $\vec{Q}=(h00)$ and $\vec{Q}=(hh0)$ Brillouin zones in which the diffuse scattering extends mainly parallel to $\vec{Q}$. The only difference between the contours near (100) and (110) appears to be in the orientation of the triangular regions of diffuse scattering, which point in toward (100) but away from (110). Data taken near (100) at 650 K are displayed in Fig. 2(b).[28] At this temperature the diffuse scattering intensities, shown using a linear gray scale, are much weaker than those of the butterfly pattern at 300 K. We further note that the intensities increase (become darker) from left to right in panels (b) and (c), which corresponds to increasing Q. Given the $(\vec{Q}\cdot\vec{u})^2$ dependence of the neutron diffuse scattering cross section, this intensity signature implies the presence of some short-range correlated displacements $\vec{u}$ since otherwise, if $u=0$, there would be no Q dependence. Thus the weak diffuse scattering is not solely due to CSRO.

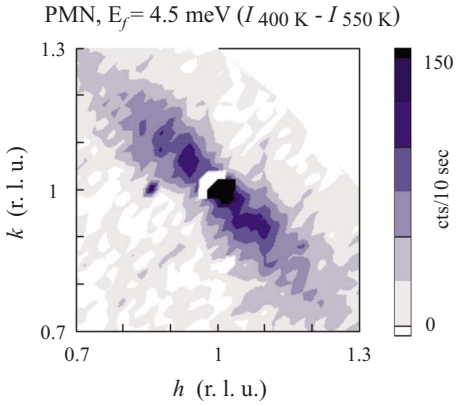

FIG. 3. (Color online) Contour plot of the difference in diffuse scattering intensity near (110) measured at 550 and 400 K. The result is the characteristic figure 8 pattern, observed previously by Vakhrushev *et al.* (Ref. 40).

In Fig. 3 we plot the difference between the diffuse scattering intensities measured near $\vec{Q}=(110)$ at 400 and 550 K. The resulting contours approximately reproduce the "figure 8" pattern observed previously by Vakhrushev *et al.*[40] and indicate that the ellipsoidal diffuse scattering has a strong temperature dependence. By contrast, the bow-tie-shaped diffuse scattering is effectively subtracted out in this analysis, which confirms that it has little to no temperature dependence. Thus the high-temperature diffuse scattering is not associated with the Burns temperature T_d or with the formation of long-range polar correlations below T_c. We note that such a strictly incoherent treatment of the high-temperature (CSRO) and low-temperature (PNR) components of the total diffuse scattering, as described here, ignores the inevitable cross terms that must exist between them. On the other hand, if the high-temperature scattering does arise primarily from CSRO, then it should be largely independent of the ionic displacements that give rise to the butterfly-shaped diffuse

scattering (PNR) below T_d. The relative weakness of the high-temperature diffuse scattering compared to that at low temperatures also suggests such cross terms should be weak, and this appears to be supported by the simple subtraction analysis presented in Fig. 3 in that one effectively recovers the ellipsoidal (not bow-tie) intensity contours. For this reason we believe it is a reasonable first approximation to treat the two diffuse scattering components as being nearly independent.

We extended the diffuse scattering measurements to temperatures well above T_d using PMN crystal 4, which we reserved for very high-temperature experiments. Previous data taken on PMN and PZN crystals heated to 1000 K revealed significant evidence of sample decomposition, so we limited our measurements to 900 K. Diffuse scattering intensity contours at 900 K for the (100) and the (300) Brillouin zones are presented in Figs. 2(c) and 2(d), respectively. Although the diffuse scattering near (100) is quite weak, it is consistent with the bow-tie geometry observed in Fig. 2(b) at 650 K. We exploited the Q^2 dependence of the neutron diffuse scattering cross section to obtain higher intensity by using thermal neutrons to access (300). The (300) diffuse scattering intensity contours are shown in Fig. 2(d), where the bow-tie pattern observed at 650 K is still present at 900 K. The contours are truncated for $h>3.02$ rlu because of a mechanical limit on the maximum scattering angle available on BT9, but the triangular region on the low-Q side of (300) is clearly evident. That the bow-tie-shaped diffuse scattering persists to such high temperature provides what is perhaps the most convincing evidence that it arises mainly from CSRO.

During the course of our measurements we noticed that the diffuse scattering in PMN crystal 4 had diminished and was noticeably weaker than that in PMN crystal 5, which we had never exposed to temperatures above 650 K. We also observed a broad ring of scattering passing directly through $\vec{Q}=(300)$, which is shown in Fig. 2(d). This feature was never observed prior to heating this crystal to 900 K. Given the length of time spent at high temperatures, this feature most likely corresponds to a powder ring arising from partially decomposed regions of PMN crystal 4, which had turned entirely black after exposure to high temperatures. These regions do not affect any other data presented in this paper because the 900 K measurements on PMN crystal 4 were the last ones performed on this sample. Therefore the powder ring appears only in Fig. 2(d).

It is instructive to compare these results with those on PMN-60%PT, a composition that lies well beyond the morphotropic phase boundary and undergoes a first-order ferroelectric transition from a cubic to a tetragonal phase near 540 K. An extensive study of this material using neutron and high-energy x-ray scattering methods found no sign of the strong butterfly-shaped diffuse scattering at low temperatures.[35] This result lends further support to our association of the strong temperature-dependent diffuse scattering with the PNR, which is absent in PMN-60%PT. Neutron measurements on PMN-60%PT do, however, reveal the presence of bow-tie-shaped diffuse scattering intensity contours at all temperatures studied, which supports the identification of such diffuse scattering with chemical short-range order

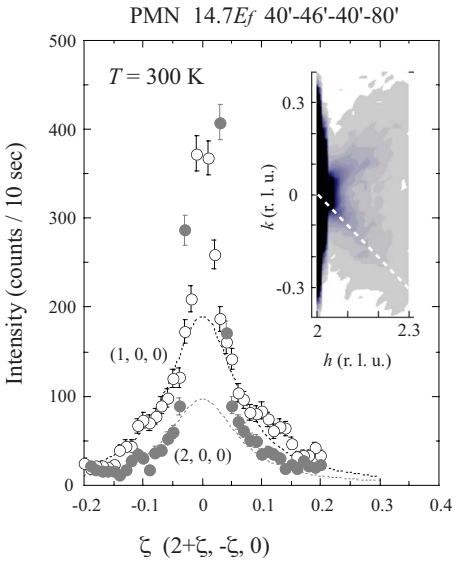

FIG. 4. (Color online) Diffuse scattering intensity measured on BT9 at 300 K as a function of reduced momentum transfer relative to (100) (open circles) and (200) (solid circles). The dotted lines isolate the diffuse scattering component from the Bragg peak. The inset shows the orientation of the scan relative to the familiar butterfly pattern measured near (200) at 100 K.

between cations on the B site of the PMN perovskite ABO_3 structure. This picture is supported by theoretical work[48] as well as ^{93}Nb NMR,[49] electron microscopy,[50] and polarized Raman scattering[51] measurements. All of these studies suggest that there is no temperature dependence to the bow-tie-shaped diffuse scattering below $\approx$1000 K, which is consistent with our results on PMN over the extended temperature range.

During our study of PMN we discovered that the diffuse scattering near (200) is not as weak as previously believed.[17,40,42,52] To confirm this finding, we made detailed measurements of the diffuse scattering intensity near (200) at 300 and 100 K along a trajectory in reciprocal space that follows one wing of the butterfly intensity contour; this is shown by the dashed line in the inset of Fig. 4. The results of the 300 K scan are compared to an identical scan measured in the (100) zone, both of which are shown in Fig. 4. These data demonstrate that the (100) diffuse scattering cross section, represented by the dotted lines passing through the open circles, is substantially larger than that at (200), designated by the solid circles. This result supports the model of Hirota *et al.*[52] in which the (unexpectedly) weak (200) diffuse scattering cross section observed in PMN and other relaxors can be explained by the presence of a uniform shift or displacement of the PNR relative to the nonpolar cubic matrix along the direction of the local PNR polarization. Indirect evidence for the existence of this shift has been obtained from neutron scattering measurements of the anisotropic response of the diffuse scattering in PZN-8%PT to an electric field applied along the [001] direction.[24]

Figure 5 shows diffuse scattering intensity contours measured on BT9 at 100, 300, and 600 K near (200); these data illustrate that the (200) diffuse scattering intensity follows the same temperature dependence as that measured in other

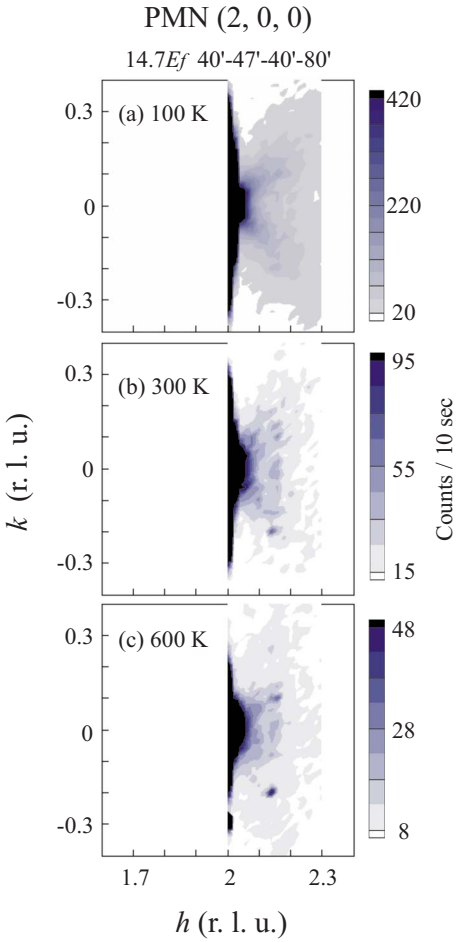

FIG. 5. (Color online) Diffuse scattering contours measured on BT9 near (200) are shown at (a) 100, (b) 300, and (c) 600 K.

Brillouin zones, where the diffuse scattering is much stronger. As the temperature is raised the diffuse scattering intensity decreases in the same manner as that previously measured and observed in the (100), (110), and (300) Brillouin zones. This proves that the diffuse scattering measured at (200) has the same origin as that in other zones, i.e., that it is associated with the formation of PNR. At 600 K in panel (c) one can already see the emergence of the bow-tie-shaped diffuse scattering that is otherwise obscured by the stronger PNR-related diffuse scattering at lower temperatures. These data are important because they support the mode-coupling analysis of Stock *et al.*,[29] which assumes that the diffuse scattering in PMN in the (200) and (220) Brillouin zones is much weaker than that in the (110) zone. Thus we emphasize that while the neutron diffuse scattering cross section near (200) is not zero, it is small and consistent with previous structure factor calculations.

IV. DIFFUSE SCATTERING DYNAMICS: REASSESSMENT OF THE BURNS TEMPERATURE

The reciprocal space geometry of the strong diffuse scattering in PMN was first characterized using x-ray diffraction and was consistent with the neutron scattering data we have

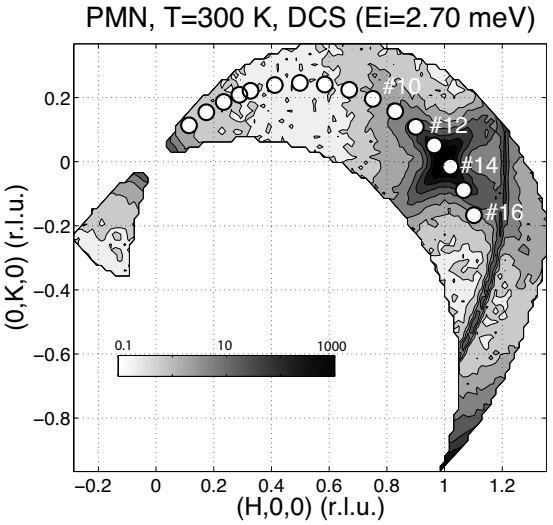

FIG. 6. Diffuse scattering intensity contours in PMN measured on the NCNR DCS near (100) are plotted on a logarithmic gray scale at 300 K. Open circles represent the reciprocal space locations of the detectors of the high-flux backscattering spectrometer relative to the butterfly-shaped intensity contours. Each open circle is a separate detector, and the detector numbers are indicated. These DCS data are taken from Xu *et al.* (Ref. 18).

presented here.[16,17] The energy resolution provided by x-ray diffraction ($\delta E \approx 1000$ meV) is typically much broader than that of thermal neutrons ($\delta E \approx 1$ meV); thus it was assumed that the strong diffuse x-ray scattering originated from low-energy, soft, TO phonons that were captured by the large energy resolution.[17,53] However the cold neutron data of Hiraka *et al.*[28] provide a much narrower elastic energy resolution of ≈0.12 meV HWHM and show, unambiguously, that the diffuse scattering cross section contains a component that is static on time scales of at least ~6 ps below 420 K as illustrated in Fig. 1. This result was subsequently confirmed on a separate PMN crystal by the neutron study of Gvasaliya *et al.*[54] which employed comparable energy resolution. Hence the observed strong diffuse scattering cannot simply be the result of a soft low-lying TO phonon. The TO mode must condense and/or broaden sufficiently to produce the elastic diffuse scattering cross section observed by Hiraka *et al.*[28] Such a scenario is in fact suggested by the corresponding thermal neutron data taken on BT9 using a somewhat coarser energy resolution of ≈0.50 meV HWHM. As shown in Fig. 1, an apparent elastic diffuse scattering cross section is observed up to temperatures as high as 650 K.

Motivated by these results, we looked for evidence of a dynamic component of the strong diffuse scattering using the NCNR HFBS, which provides an elastic energy resolution $\delta E = 0.4$ μeV HWHM. We oriented PMN crystal 4 in the (*hk*0) scattering plane, which is the same geometry used in the triple-axis study of Hiraka *et al.*[28] Figure 6 displays the resulting locations of each of the 16 HFBS detectors relative to the butterfly-shaped diffuse scattering pattern at (100) measured previously using the NCNR disk chopper spectrometer (DCS).[18] From this figure it can be seen that detectors 10–16 sample different parts of the wings of the strong diffuse scattering. In particular, detectors 13 and 14 lie close

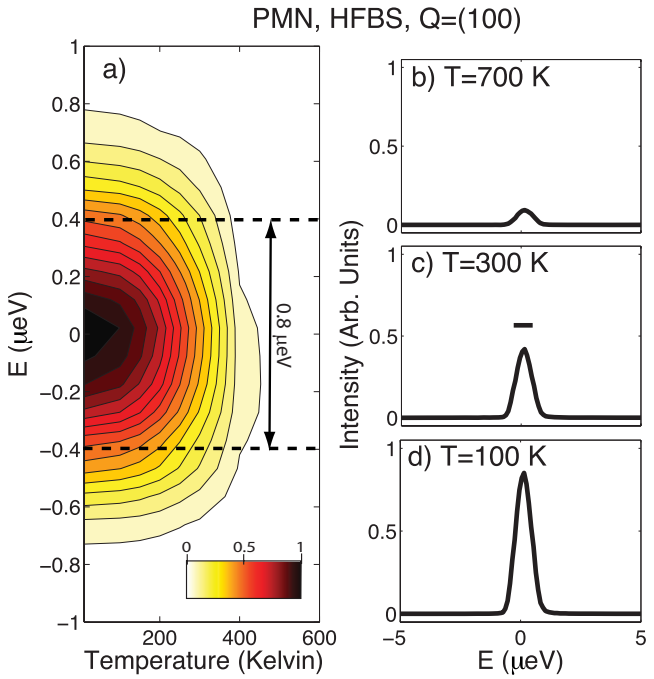

FIG. 7. (Color online) (a) Contour plot of the diffuse scattering intensity measured on the HFBS as a function of energy transfer and temperature. Contours are shown on a linear intensity scale; dashed lines indicate the FWHM of the peak linewidth at each temperature. Data were summed over detectors 10–16 as illustrated in Fig. 6. Panels (b)–(d) show inelastic scans at 700, 300, and 100 K. The horizontal bar in panel (c) represents the instrumental FWHM elastic energy resolution ($2\delta E$).

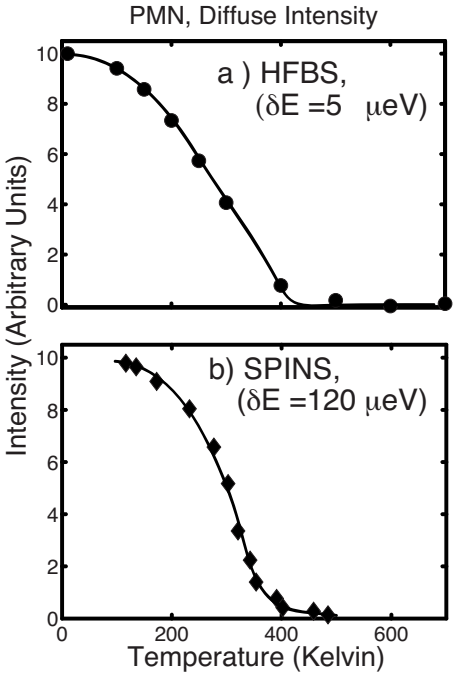

FIG. 8. (a) Temperature dependence of the diffuse scattering measured on the HFBS; data are integrated in energy from ± 5 μeV and in Q over detectors 10–16 as illustrated in Fig. 6. (b) Temperature dependence of the diffuse scattering intensity measured on SPINS at (1.05,0.95,0) by Hiraka *et al.* (Ref. 28). The SPINS energy resolution of $\delta E = 120$ μeV HWHM provided the energy integration.

to the (100) Bragg peak. Because the instrumental Q resolution of the HFBS is relatively poor, we checked for the presence of Bragg contamination in the integration analysis by removing contributions from detectors 13 and 14. This did not change any of the results. Moreover the PMN study by Wakimoto *et al.*[55] showed the (202) Bragg peak intensity changes by less than 10% between 50 and 300 K. Therefore, in the following analysis we have integrated the intensity from detectors 10–16.

The energy dependence of the diffuse scattering as a function of temperature is illustrated in Fig. 7. Panel (a) shows a color contour plot of the peak linewidth in energy as a function of temperature after subtraction of a high-temperature background. This background was taken to be the average of the intensity measured at 600 and 700 K because no strong diffuse scattering is observed with either cold neutron triple-axis or neutron backscattering methods at these temperatures. The distance between the dashed lines represents the measured energy width (full width at half maximum) as a function of temperature. Typical energy scans are displayed in panels (b)–(d) at 700, 300, and 100 K, respectively. We see that the peak centered at $\hbar\omega = 0$ is equal to the instrumental energy resolution $\delta E = 0.4$ μeV HWHM at all temperatures. Based on this analysis, we conclude that the strong diffuse scattering is elastic on time scales of at least $\tau \approx \hbar/\delta E \sim 2$ ns. Our results are thus consistent with the neutron-spin echo study on PMN of Vakhrushev *et al.*[41]

Figure 8(a) shows the temperature dependence of the diffuse scattering intensity integrated over ± 5 μeV. These data are compared to those measured on PMN crystal 5 using the cold neutron spectrometer SPINS, which are plotted in panel (b). That the temperature dependences from the backscattering and SPINS measurements agree within error in spite of a 300-fold (120 μeV/0.4 μeV) difference in energy resolution proves that static short-range polar order first appears at much lower temperatures than has been understood from previous data measured with much coarser energy resolution. These data thus demand a revised value for the Burns temperature: $T_d = 420 \pm 20$ K. We mention, however, that if the diffuse scattering energy width obeys an Arrhenius or some power law form, which has been suggested for spin glasses in Ref. 56, then a more detailed analysis based on data taken closer to the onset of the diffuse scattering at 420 K will be required to confirm (or reject) the existence of such alternative dynamic contributions to the diffuse scattering energy width.

To gain a better understanding of the apparent quasielastic nature of the diffuse scattering, we examined the temperature dependence of the low-energy TA modes in greater detail. In particular we focused on measurements of the temperature-dependent broadening of the transverse acoustic phonon over a range of reduced wave vectors q that approach the zone center ($q = 0$). These data are discussed in Sec. V.

V. TA AND TO PHONONS: EFFECTS OF THE PNR

An extensive series of inelastic measurements was made on both PMN crystals 4 and 5 in the (110) Brillouin zone

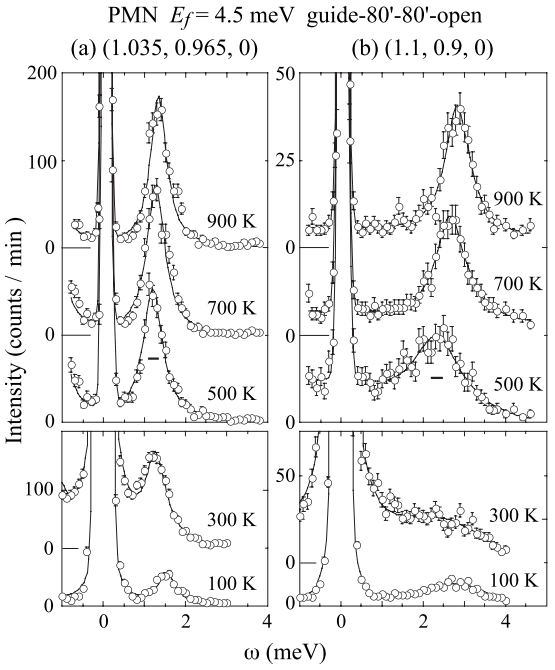

FIG. 9. TA phonon line shapes in PMN measured on SPINS with cold neutrons at $\vec{Q}=(1.035,0.965,0)$ and (1.1,0.9,0) from 100 to 900 K.

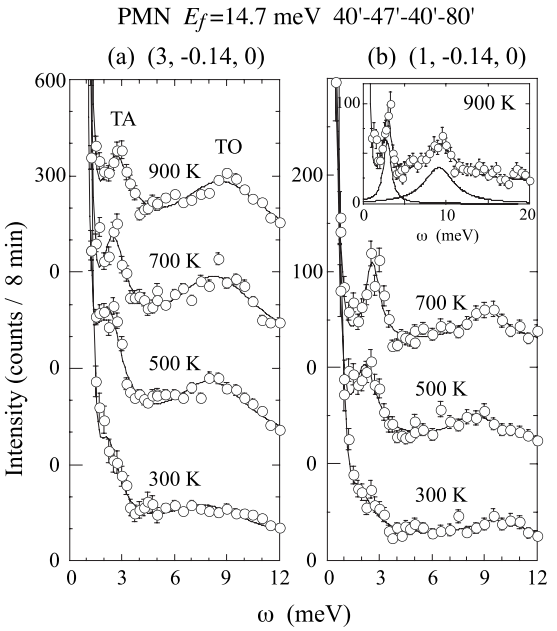

FIG. 10. TA and TO phonon line shapes in PMN measured on BT9 with thermal neutrons near the waterfall wave vector at $\vec{Q}=(3,-0.14,0)$ and $(1,-0.14,0)$ from 300 to 900 K.

using the SPINS spectrometer in an effort to map out the temperature dependence of the TA mode for reduced wave vectors $q \ll q_{wf}$ and $q \approx q_{wf}$, where $q_{wf}=0.14$ rlu ≈ 0.2 Å^{-1} is the wave vector associated with the so-called "waterfall" effect, and below which the long-wavelength soft TO modes in PMN, PZN, and PZN-8%PT are observed to broaden markedly at temperatures below T_d.[27,57–60] This zone was chosen because the TA phonon dynamical structure factor for (110) is much larger than that for (100). The TA phonon energy line shapes were studied at two very different values of the reduced wave vector q, measured relative to the (110) zone center, for temperatures between 100 and 900 K. These data are presented in Fig. 9. The data shown on the left-hand side of this figure correspond to $\vec{Q}=(1.035,0.965,0)$ or $q=\sqrt{2}\times 0.35$ rlu=0.05 rlu=0.077 Å^{-1}, which is less than half of q_{wf}. These data show that the TA line shape at this small wave vector remains sharp and well defined at all temperatures and has an intrinsic energy width that is larger than the instrumental resolution (shown by the small solid horizontal bar at 500 K). By contrast, the data on the right-hand side of Fig. 9 correspond to $\vec{Q}=(1.1,0.9,0)$ or $q=\sqrt{2}\times 0.10$ rlu=0.14 rlu=0.22 Å^{-1}, which is nearly equal to q_{wf}. In this case it is quite evident that the TA line shape broadens dramatically, becoming increasingly ill-defined below T_d, especially at 300 K, but then sharpens at lower temperature, e.g., at 100 K. This behavior is the same as that observed for the soft zone-center TO mode in PMN by Wakimoto *et al.*[27] measured at (200).

In addition to these cold neutron measurements of the TA mode using SPINS, other measurements were made using thermal neutrons on BT9 to characterize the TO mode line shapes for reduced wave vectors $q \approx q_{wf}$ from 300 to 900 K. In these experiments data were taken using a water-cooled furnace with PMN crystal 4 in both the (300) and (100) Brillouin zones for $q=q_{wf}=0.14$ rlu and are shown in Fig. 10. As can be seen on the left-hand side of this figure, both the TA and TO modes are well defined at 900 K. The scattering intensity below 1–2 meV increases sharply because of the comparatively coarser energy resolution intrinsic to BT9 (≈0.5 meV HWHM), which uses thermal neutrons, compared to that on SPINS. Even so, the TA mode is easily seen at both 900 and 700 K. However at 500 K the TA mode is less well defined. This occurs in part not only because the mode has broadened but also because the low-energy scattering has increased, which results from the onset of the strong diffuse scattering due to the PNR. At 300 K the TA mode is nearly indistinguishable from the sloping background, and the TO mode has become significantly damped. One also sees a gradual softening of the TO mode from 900 down to 300 K that is of order 1–2 meV. The same data were taken in the (100) zone, which appear in the right-hand portion of Fig. 10. Essentially the same trends are observed in this zone, with the TA mode again becoming almost indistinguishable from background at 300 K. One difference is that the TA mode is better separated at all temperatures from the steep increase in scattering seen at low energies. These data are consistent with the conjecture of Stock *et al.*[29] that the low-energy TA phonon is coupled to the diffuse scattering centered around the elastic position. The inset on the top panel on the right-hand side displays the full TA-TO phonon spectrum at 900 K out to 20 meV.

The squares of the energies of both the TA and TO modes presented in the two previous figures are plotted versus temperature in Fig. 11. This is done to draw attention to the similarity between the low-energy lattice dynamics of PMN and the behavior expected for a conventional ferroelectric, for which the soft-mode frequency squared ω^2 varies linearly

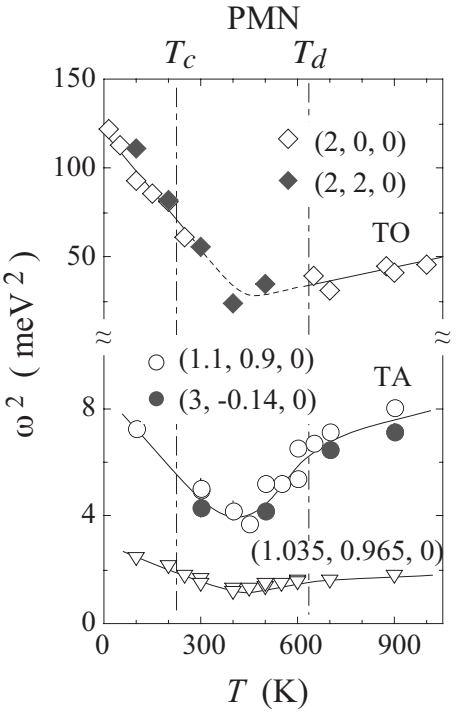

FIG. 11. The square of the phonon energy is plotted versus temperature for the zone-center TO modes measured at (200) (open diamonds) and (220) (solid diamonds) taken from Wakimoto *et al.* (Ref. 27) and Stock *et al.* (Ref. 29), as well as for three TA modes measured at (1.035,0.965,0) (open triangles), (1.1,0.9,0) (open circles), and (3,−0.14,0) (solid circles). Linear behavior is consistent with that expected for a conventional ferroelectric soft mode.

with $(T-T_c)$. Data for the zone-center soft mode measured at (200) and (220) have been taken from Wakimoto *et al.*[27] and Stock *et al.*[29] and added to the top of Fig. 11 for ease of comparison. The data taken by Wakimoto *et al.*[27] are based on energy scans measured at constant Q at the zone center, whereas Stock *et al.*[29] determined the zone-center TO energies by extrapolating from data obtained at nonzero q. The extrapolation technique permits phonon energies to be extracted in the temperature range where the zone-center TO mode is heavily damped. These values for the zone-center TO phonon energy have been confirmed by infrared spectroscopy.[61] What this figure immediately reveals, then, is a surprising ferroelectric character of the zone-center TO mode above T_d and below T_c and a corresponding change in the behavior of the TA mode energy that is bracketed by the same two temperature scales, which are denoted by the two vertical dashed-dotted lines. We note that no such change in the acoustic phonons was observed in PMN-60%PT where PNR and the associated strong diffuse scattering are absent; therefore the softening of the TA mode is directly related to the development of PNR.[35] A further interesting feature is the minimum that is present in all of these data near 420 K, which is the same temperature at which the strong diffuse scattering first appears when measured with high-energy resolution, namely, the revised value of the Burns temperature. Therefore, the onset of the diffuse scattering is directly associated with the softening of the TO mode; this is yet further evidence that it is associated with the formation of static short-range polar correlations.

It is very important to note that the square of the TA phonon energy measured at $\vec{Q}=(1.1,0.9,0)$, which corresponds to $q\sim 0.14$ rlu, shows a much more pronounced minimum at 420 K than does that measured at $\vec{Q}=(1.035,0.965,0)$, which corresponds to $q\sim 0.05$ rlu. This shows that long-wavelength TA phonons exhibit a much weaker response to the formation of static short-range polar correlations. This can be understood in terms of a simple physical picture in which those phonons with wavelengths comparable to the size of the PNR are strongly affected (damped) by the PNR whereas longer wavelength phonons simply average over the PNR and are thus not affected by the presence of static short-range polar correlations. This idea was previously proposed to explain the anomalous damping of the TO mode for wave vectors $q\leq q_{wf}$ near the zone center.[57] However, no strong diffuse scattering is seen in PMN-60%PT and thus no PNR are present, even though the anomalous TO broadening is still observed; hence this TO broadening, which gives rise to the waterfall effect, cannot be associated with the presence of static short-range polar correlations. On the other hand, the idea that the acoustic phonons are affected by PNR is confirmed by the absence of any such acoustic phonon broadening in PMN-60%PT. Thus PNR have a significant effect on the low-energy acoustic phonons over a limited range of reduced wave vectors that may be related to the size of the PNR. In light of the diffuse and inelastic scattering data that have been analyzed so far, we now turn to the detailed measurement of the thermal expansion in PMN.

VI. THERMAL EXPANSION: INVARLIKE EFFECT BELOW T_d

A variety of experimental techniques has been used to measure the thermal expansion in both single crystal and powder samples of PMN, which includes x-ray diffraction, laser dilatometry, and neutron diffraction.[62–64] Here we present extremely high q-resolution neutron measurements ($\delta q\approx 0.0005$ rlu$=0.0008$ Å^{-1} HWHM) of the cubic unit cell lattice parameter a of PMN crystal 5 using the special triple-axis configuration described in the experimental section. This configuration, which employs a perfect single crystal of Ge as analyzer, also provides an exceptional energy resolution $\delta E\approx 5-10$ μeV HWHM. The resulting data are plotted in Fig. 12 in terms of the strain a/a_0-1, where a_0 is the lattice parameter at 200 K. Measurements were made on heating from 30 to 580 K using a closed-cycle ^{4}He refrigerator after having first cooled to 30 K. X-ray data measured by Dkhil *et al.*[64] on a single crystal of PMN, shown as open squares, are provided for comparison.

Several features are interesting to note. First, at low temperature the system exhibits an invarlike effect in which the cubic lattice parameter changes by less than 0.001 Å; indeed, the data below 320 K are consistent with a thermal expansion of zero. At higher temperatures, however, the average thermal expansion is 2.5×10^{-5} K^{-1}. That these disparate regions of null and high rates of thermal expansion bracket the revised value for the Burns temperature suggests

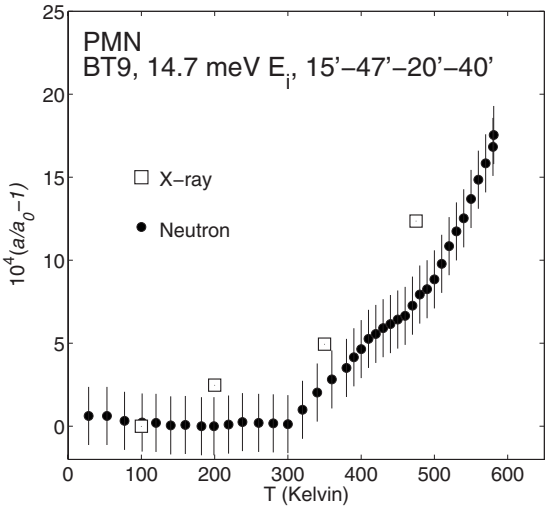

FIG. 12. Lattice strain of single crystal PMN derived from the (220) Bragg reflection measured from 30 to 580 K on BT9. Data were obtained on heating using a perfect Ge(004) analyzer, an incident neutron energy E_i=14.7 meV, and horizontal beam collimations of 15′-47′-S-20′-40′ to obtain extremely high q resolution. X-ray data from Dkhil *et al.* (Ref. 64) are indicated by the open squares for comparison.

that a direct connection exists between the onset of static short-range polar correlations and the structural properties of PMN. This behavior seems to be consistent with that of PZN, which also exhibits an increase in the thermal expansion at temperatures above that where the diffuse scattering first appears.[65]

There is ample evidence of similar behavior reported by other groups in samples of PMN and PMN-xPT. A low-temperature invarlike effect was observed in single crystal PMN-10%PT, where a transition to a high rate of thermal expansion was found at 400 K; the thermal expansion for this sample at high temperature is 1×10^{-5} K^{-1}, which is very close to that measured here.[66] The x-ray study of ceramic samples of PMN by King *et al.*[67] also shows a transition between low and high rates of thermal expansion but larger values for both. X-ray and neutron work conducted by Bonneau *et al.*[68] on PMN powders yielded onset temperatures and values for the thermal expansion consistent with our single crystal measurements. Finally, an invar effect was also observed in the laser dilatometry study by Arndt and Schmidt[63] on a ceramic sample of PMN, which covered a range from 300 to 800 K.

Even though there is a general trend toward a larger thermal expansion for temperatures above that where the diffuse scattering is onset, there is some sample dependence and some differences between powders and single crystals. As noted by Ye *et al.*,[69] powder measurements of PMN yield a different slope for the thermal expansion measurements than do those of Dkhil *et al.*[64] Also, studies using neutron strain scanning techniques found different thermal expansion coefficients as a function of depth in single crystal samples.[70,71] Therefore, part of the discrepancy observed between different samples may be associated with surface effects. In this regard, we also note the presence of a change in the slope of the strain curve between 400 and 500 K; since this change is not observed in other PMN studies, we believe this feature to be sample dependent and thus extrinsic.

The phase-shifted model of polar nanoregions proposed by Hirota *et al.*[52] provides a plausible starting point from which to understand the anomalous invarlike behavior in PMN below the Burns temperature T_d. This model is based on the observation that the Pb, Mg, Nb, and O ionic displacements obtained from the diffuse scattering measurements of Vakhrushev *et al.*[40] on PMN can be decomposed into a center-of-mass conserving component, consistent with the condensation of a soft transverse optic mode and a uniform scalar component, corresponding to an acoustic phase shift. In so doing Hirota *et al.*[52] were able to reconcile the discrepancies between the structure factors of the diffuse scattering and the soft TO modes and, in particular, to explain the weakness of the diffuse scattering intensity observed in the vicinity of the (200) Bragg peak.[52] The idea that the PNR are uniformly displaced with respect to the underlying cubic lattice in a direction parallel to the PNR polarization has already been used by Gehring *et al.*[24] to explain the persistence of the strong diffuse scattering in a single crystal of PZN-8%PT against large electric fields applied along [001]. In that study it was shown that the diffuse scattering near (003), which measures the projections of the ionic displacements along [001], decreases under an external [001] field as expected. By contrast, the diffuse scattering near (300), which measures the projections of the ionic displacements along [100], i.e., perpendicular to the field direction, remains unaffected even for field strengths up to 10 kV/cm. Thus a uniform polar state is not achieved. This surprising behavior can be understood if one assumes that the electric field applied along [001] removes or reduces the PNR shifts along [001] while preserving those along [100]. The diffuse scattering should then decrease anisotropically with field, as is observed. In the context of the invarlike behavior of PMN below T_d, we speculate that such uniform shifts of the PNR could effectively stabilize the lattice against subsequent thermal expansion at lower temperature. Such a scenario is consistent with the fact that both PMN-10%PT and PMN-20%PT retain cubic structures down to low temperature when examined with high q-resolution neutron diffraction methods.[66,72]

VII. DISCUSSION AND CONCLUSIONS

We have presented a comprehensive neutron study of the diffuse scattering in the relaxor PMN. We have greatly extended the time scales of previous neutron measurements by taking data on three different spectrometers, BT9, SPINS, and the HFBS, which provide elastic energy resolutions of 500, 120, and 0.4 μeV HWHMs, respectively. While the backscattering data represent a 300-fold improvement in energy resolution over those obtained by Hiraka *et al.*[28] on SPINS, both yield an onset temperature of 420 ± 20 K for the diffuse scattering. This indicates that the PNR in PMN are static on time scales of at least 2 ns below 420 K but are apparently dynamic at higher temperatures. Thus the true Burns temperature in PMN, which was originally interpreted

by Burns and Dacol[5] as the condensation temperature of static regions of local, randomly oriented, nanometer-scale polarization, is 420 ± 20 K, not 620 K. Independent evidence of the existence of purely dynamic, short-range, polar correlations has been reported in PMN-55%PT, a composition with no strong diffuse scattering and thus no static PNR, by Ko *et al.*[73] who observed phenomena that are typically related to the relaxation of dynamic PNR. These include significant Brillouin quasielastic scattering, a softening of the longitudinal acoustic phonon mode, and a deviation of the dielectric constant from Curie-Weiss behavior over an 80 K temperature interval above T_c.

Previous measurements of the temperature dependence of the neutron diffuse scattering have been extended in this study to 900 K, well above T_d. In so doing we have unambiguously established the existence of two types of diffuse scattering based on the observation of two markedly different temperature dependencies, one of which vanishes at T_d and one of which does not. We associate the strong, temperature-dependent, diffuse scattering with the formation of static, short-range, polar correlations (PNR) because of its well documented response to an external electric field and because it first appears at the same temperature at which the soft (polar) TO mode reaches a minimum in energy. We associate the weak, temperature-independent, diffuse scattering, which shows no obvious change across either T_c or T_d, with chemical short-range order because it persists to extremely high temperature. We further confirm the observations of Hiraka *et al.*,[28] who first characterized the distinctly different reciprocal space geometries of both types of diffuse scattering, and we show that the bow-tie shape of the weak diffuse scattering persists up to 900 $\mathrm{K} \gg T_d$.

Key effects of the strong, temperature-dependent, diffuse scattering and thus of the PNR on the low-energy lattice dynamics of PMN are also highlighted in this study. The neutron inelastic measurements on PMN-60%PT by Stock *et al.*[35] prove conclusively that PNR cannot be the origin of the anomalous broadening of long-wavelength TO modes observed in PMN, PZN, and other compounds, also known as the waterfall effect, because PMN-60%PT exhibits the same effect but no strong diffuse scattering (no PNR). By contrast, many studies have shown that PNR do broaden the TA modes in PMN (Refs. 14, 15, and 29) and in PZN-*x*PT,[42] but that such effects are absent in compositions with no PNR such as PMN-60%PT.[35] Our cold neutron data show that these effects are q dependent. Whereas long-wavelength TA modes with reduced wave vectors $q \ll 0.2$ Å^{-1} remain well defined and exhibit a nearly constant energy width (lifetime) from 100 to 900 K, shorter wavelength TA modes with reduced wave vectors $q \approx 0.2$ Å^{-1} broaden substantially, with the maximum broadening occurring at $T_d = 420$ K. This result motivates a very simple physical picture in which only those acoustic phonons having wavelengths comparable to the size of the PNR are significantly scattered by the PNR; acoustic modes with wavelengths much larger than the PNR are largely unaffected because they simply average over the PNR. Models describing this effect have been discussed elsewhere.[29] In particular, very recent work by Xu *et al.*[74] has revealed the presence of a phase instability in PZN-4.5%PT that is directly induced by such a PNR-TA phonon interaction. This is shown to produce a pronounced softening and broadening of TA modes in those zones where the diffuse scattering is strong and provides a natural explanation of the enormous piezoelectric coupling in relaxor materials.[74]

In addition, we have performed neutron measurements of the thermal expansion with extremely high q and $\hbar\omega$ resolutions over a broad temperature range extending well below T_c and far above $T_d \sim 420$ K. In agreement with many other studies, our single crystal samples of PMN exhibit little or no thermal expansion below T_d, behavior that is reminiscent of the invar effect, but an unusually large thermal expansion coefficient of 2.5×10^{-5} K^{-1} above T_d, where the strong diffuse scattering is absent. The crossover between null and large coefficients of thermal expansion coincides closely with T_d, which suggests that the appearance of static PNR strongly affects the thermal expansion in PMN and thus provides a structural signature of the formation of short-range polar correlations in zero field. The model of uniformly displaced, or phase-shifted, PNR proposed by Hirota *et al.*,[52] which successfully predicts the anisotropic response of the strong diffuse scattering to an electric field, offers a simplistic, yet plausible, framework in which to understand this anomalous behavior.

Finally, it is satisfying to note that the revised value of $T_d = 420 \pm 20$ K is consistent with the dielectric susceptibility data of Viehland *et al.*,[75] from which a Curie-Weiss temperature $\Theta = 398$ K was derived. Such good agreement between T_d and Θ solidifies our identification of the strong diffuse scattering with the condensation of the soft TO mode, which reaches a minimum frequency at $T_d = 420$ K. However this begs the question of how one should interpret the original Burns temperature of ~ 620 K. At present there are two broadly divergent opinions on this issue, one of which considers ~ 620 K to be a meaningful temperature scale in PMN and one of which does not. As it turns out, this debate is closely tied to another on how many temperature scales are needed to describe the physics of relaxors. We offer no final resolution to this discussion. Instead, we close our paper with a brief summary of the primary studies supporting these contrasting points of view, which is by no means comprehensive, so that the readers may draw their own conclusions.

A number of experimental studies report evidence of either structural or dynamic changes in PMN in the temperature range of 600–650 K, starting with the optical index of refraction measurements of Burns and Dacol.[5] Siny and Smirnova[76] were the first to observe strong first-order Raman scattering in PMN at high temperatures, which, being forbidden in centrosymmetric crystals, implied the presence of some type of lattice distortion. In 2002 Vakhrushev and Okuneva[77] calculated the probability density function for the Pb ion in PMN within the framework of the spherical layer model using x-ray powder diffraction data. It was shown that this probability density evolves from a single Gaussian function centered on the perovskite A site to a double Gaussian form between 635 and 573 K and that the positions of maximum density for the lead ion follow a power law $(T_d - T)^{0.31}$ with $T_d = 635$ K. This picture was developed further by Prosandeev *et al.* within a model that ascribed the changes in the lead probability density function and subtle variations in the thermal expansion near 620 K to a crossover

from soft-mode to order-disorder dynamics.[78] In 2004 Egami *et al.*[79] first proposed that at very high temperatures the vibrations of the oxygen octahedra are sufficiently faster than those of the Pb ions that, on average, a high-symmetry local environment is obtained, whereas at temperatures below ~680 K the Pb and O ions become dynamically correlated. This led to the subsequent reinterpretation of the Burns temperature (~600 K) as being the point below which dynamic PNR first form, which was based on the dynamic PDF measurements of Dmowski *et al.*[80] obtained with an elastic energy resolution of 4 meV at six temperatures (680, 590, 450, 300, 230, and 35 K). Interestingly, after integrating their data from −5 to +5 meV, Dmowski *et al.*[80] saw evidence of a third temperature scale in PMN of order 300 K, and thus distinct from both $T_c \sim 210$ K and $T_d \sim 600$ K, which they associated with the formation of static PNR. Similar ideas have very recently been put forth by Dkhil *et al.*[64] based on extremely interesting acoustic emission and thermal expansion measurements and also in a general summary written by Toulouse.[81,82]

A different approach was taken by Stock *et al.*[83] who proposed a unified description of the lead-based relaxors on the basis of striking similarities between PMN and the Zn-analog PZN, both of which display strong, temperature-dependent, diffuse scattering, identical soft-mode dynamics, yet no long-range structural distortion at low temperature in zero field.[84] Arguing by analogy with magnetic systems, Stock *et al.*[83] considered a three-dimensional Heisenberg model with cubic anisotropy in the presence of random fields in which the Heisenberg spin corresponds to the local ferroelectric polarization, the cubic anisotropy represents the preferential orientation of the polarization along the ⟨111⟩ axes, and the isotropic random magnetic field corresponds to the randomly oriented local electric fields that originate from the varying charge of the *B*-site cation. Following a suggestion by Aharony,[85] Stock *et al.*[83] considered the case where the Heisenberg term dominates over the random field term, and the cubic anisotropy term is the weakest of the three. In this picture there would be just two distinct, static, temperature scales. For $T > T_d$, the cubic anisotropy is irrelevant and therefore the system should behave like a Heisenberg system in a random field. In this case the excitation spectrum is characterized by Goldstone modes and therefore no long-range order is expected in the presence of random fields.[85] Instead the system forms polar nanoregions in a paraelectric background. The second temperature scale T_c appears at low temperatures where the cubic anisotropy term becomes important, and in this limit the system should resemble an Ising system in the presence of a random field. This model thus explains the local ferroelectric distortion characterized by the recovery of the soft-optic mode and, although a 3D Ising system in equilibrium should display long-range order in the presence of small random fields, as is observed in magnetic systems, nonequilibrium effects with long time scales become dominant. The presence of such nonequilibrium effects may explain the lack of long-range ferroelectric order in PMN and PZN, as well as the history dependence of physical properties such as the linear birefringence. The phase-shifted nature of the polar nanoregions may also create another energy barrier against the ordered phase at T_c. Stock *et al.*[83] are also able to explain the physics of compounds beyond the MPB, such as PMN-60%PT, within this model, for which only one temperature scale (T_c) exists. As the Ti concentration Ti increases, the relaxor phase diagram crosses over to a ferroelectric regime, and this can be understood as an increase in the strength of the cubic anisotropy term that is simultaneously accompanied by a reduction in the random fields as must occur in the limit of pure $PbTiO_3$.[35] It should be mentioned that other studies have invoked random fields to explain the static and dynamic properties of relaxors.[86–88]

Independent of the validity of either of the two pictures summarized above, the seminal finding of our study remains that the strong diffuse scattering in PMN first appears at a temperature that depends sensitively on the energy resolution of the measurement. This fact inevitably raises interesting questions about the significance of the previous value of the Burns temperature (~620 K). If the strong diffuse scattering in PMN results from the soft TO mode, then other techniques based on x-ray diffraction, thermal neutron scattering, or neutron PDF, which provide comparatively much coarser energy resolution, will be unable to discriminate between low-energy, dynamic, short-range polar correlations and truly static ($\hbar\omega = 0$) PNR because any low-energy polar correlations will be integrated into the elastic channel by the broad energy resolution. Thus as the TO mode softens, the associated low-energy, polar, spectral weight will fall within the energy resolution at temperatures above $T_d = 420$ K, and the net result will be an artificially higher value of T_d that increases with the size of the energy resolution. This effect should be especially pronounced for phonon modes that are broad in energy (i.e., that have short lifetimes), and this is clearly the case for the soft TO mode in PMN, which exhibits a nearly overdamped line shape and a minimum frequency precisely at $T_d = 420$ K. While it is true that the structure factor of the strong diffuse scattering is inconsistent with that of the soft TO mode, the phase-shifted model of Hirota *et al.*[52] provides a way to reconcile this discrepancy. In this respect, we simply suggest that the previous value of $T_d \sim 620$ K might not represent a physically meaningful temperature scale in PMN. Future studies examining the values of T_d in other relaxor compounds with improved energy resolution are thus of interest.

Our reassessment of the Burns temperature T_d immediately clarifies an intimate relationship between the formation of static short-range polar correlations and the consequent effects on both the low-energy lattice dynamics and structure of PMN. Cold neutron triple-axis and backscattering spectroscopic methods conclusively show the existence of static short-range polar correlations only below $T_d = 420 \pm 20$ K on time scales of at least 2 ns. Thermal neutron measurements of the lattice dynamics reflect the presence of these static PNR through the presence of a distinct minimum in both the soft TO and TA mode energies, both of which occur at 420 K. The effect of PNR on the lattice dynamics is evident only for TA modes having wave vectors of order 0.2 $Å^{-1}$, a fact that could be exploited to determine the size of the PNR. At the same time an enormous change in the coefficient of thermal expansion is seen near T_d, below which the crystal lattice exhibits invarlike behavior.

ACKNOWLEDGMENTS

We would like to thank A. Bokov, Y. Fujii, K. Hirota, D. Phelan, S. Shapiro, S. Wakimoto, and G. Xu for stimulating discussions. This study was supported in part by the US-Japan Cooperative Neutron-Scattering Program, the Natural Sciences and Engineering Research Council of Canada (NSERC), the National Research Council of Canada (NRC), the Japanese Ministry of Monbu-Kagaku-shou, the RFBR under Grant Nos. 08-02-00908 and No. 06-02-90088NSF, the U.S. Department of Energy under Contract No. DE-AC02-98CH10886, the U.S. Office of Naval Research under Grant No. N00014-06-1-0166, and the NSF under Grant No. DMR-9986442. We also acknowledge the U.S. Department of Commerce, NIST Center for Neutron Research, for providing the neutron scattering facilities used in this study, some of which are supported in part by the National Science Foundation under Agreement No. DMR-0454672.

[1] Z.-G. Ye, Key Eng. Mater. **155-156**, 81 (1998).
[2] S.-E. Park and T. R. Shrout, J. Appl. Phys. **82**, 1804 (1997).
[3] A. A. Bokov and Z.-G. Ye, J. Mater. Sci. **41**, 31 (2006).
[4] B. E. Vugmeister, Phys. Rev. B **73**, 174117 (2006).
[5] G. Burns and F. H. Dacol, Solid State Commun. **48**, 853 (1983); Phys. Rev. B **28**, 2527 (1983).
[6] P. Bonneau, P. Garnier, E. Husson, and A. Morell, Mater. Res. Bull. **24**, 201 (1989).
[7] N. de Mathan, E. Husson, G. Calvarin, J. R. Gavarri, A. W. Hewat, and A. Morell, J. Phys.: Condens. Matter **3**, 8159 (1991).
[8] J. Zhao, A. E. Glazounov, Q. M. Zhang, and B. Toby, Appl. Phys. Lett. **72**, 1048 (1998).
[9] K. Hirota, S. Wakimoto, and D. E. Cox, J. Phys. Soc. Jpn. **75**, 111006 (2006).
[10] R. Blinc, V. Laguta, and B. Zalar, Phys. Rev. Lett. **91**, 247601 (2003).
[11] V. V. Shvartsman and A. L. Kholkin, Phys. Rev. B **69**, 014102 (2004).
[12] T. Egami, S. Teslic, W. Dmowski, P. K. Davies, and I.-W. Chen, J. Korean Phys. Soc. **32**, S935 (1998); T. Egami, W. Dmowski, S. Teslic, P. K. Davies, I. W. Chen, and H. Chen, Ferroelectrics **206**, 231 (1998).
[13] I.-K. Jeong, T. W. Darling, J. K. Lee, Th. Proffen, R. H. Heffner, J. S. Park, K. S. Hong, W. Dmowski, and T. Egami, Phys. Rev. Lett. **94**, 147602 (2005).
[14] A. Naberezhnov, S. B. Vakhrushev, B. Dorner, and H. Moudden, Eur. Phys. J. B **11**, 13 (1999).
[15] T. Y. Koo, P. M. Gehring, G. Shirane, V. Kiryukhin, S. G. Lee, and S. W. Cheong, Phys. Rev. B **65**, 144113 (2002).
[16] S. Vakhrushev, A. Naberezhnov, S. K. Sinha, Y. P. Feng, and T. Egami, J. Phys. Chem. Solids **57**, 1517 (1996).
[17] H. You and Q. M. Zhang, Phys. Rev. Lett. **79**, 3950 (1997).
[18] G. Xu, G. Shirane, J. R. D. Copley, and P. M. Gehring, Phys. Rev. B **69**, 064112 (2004).
[19] G. Xu, Z. Zhong, Y. Bing, Z.-G. Ye, and G. Shirane, Nature Mater. **5**, 134 (2006).
[20] M. Matsuura, K. Hirota, P. M. Gehring, Z.-G. Ye, W. Chen, and G. Shirane, Phys. Rev. B **74**, 144107 (2006).
[21] G. Xu, Z. Zhong, H. Hiraka, and G. Shirane, Phys. Rev. B **70**, 174109 (2004).
[22] S. B. Vakhrushev, A. A. Naberezhnov, N. M. Okuneva, and B. N. Savenko, Phys. Solid State **40**, 1728 (1998).
[23] C. Stock, G. Xu, P. M. Gehring, H. Luo, X. Zhao, H. Cao, J. F. Li, D. Viehland, and G. Shirane, Phys. Rev. B **76**, 064122 (2007).
[24] P. M. Gehring, K. Ohwada, and G. Shirane, Phys. Rev. B **70**, 014110 (2004).
[25] G. Xu, P. M. Gehring, and G. Shirane, Phys. Rev. B **72**, 214106 (2005).
[26] G. Xu, P. M. Gehring, and G. Shirane, Phys. Rev. B **74**, 104110 (2006).
[27] S. Wakimoto, C. Stock, R. J. Birgeneau, Z.-G. Ye, W. Chen, W. J. L. Buyers, P. M. Gehring, and G. Shirane, Phys. Rev. B **65**, 172105 (2002).
[28] H. Hiraka, S.-H. Lee, P. M. Gehring, G. Xu, and G. Shirane, Phys. Rev. B **70**, 184105 (2004).
[29] C. Stock, H. Luo, D. Viehland, J. F. Li, I. Swainson, R. J. Birgeneau, and G. Shirane, J. Phys. Soc. Jpn. **74**, 3002 (2005).
[30] J. Hlinka, S. Kamba, J. Petzelt, J. Kulda, C. A. Randall, and S. J. Zhang, J. Phys.: Condens. Matter **15**, 4249 (2003).
[31] S. N. Gvasaliya, S. G. Lushnikov, and B. Roessli, Crystallogr. Rep. **49**, 108 (2004).
[32] S. N. Gvasaliya, S. G. Lushnikov, and B. Roessli, Phys. Rev. B **69**, 092105 (2004).
[33] The study by Hlinka *et al.* (Ref. 30) employed a much narrower energy resolution of 30 μeV full width at half maximum (FWHM) than did the studies of Gvasaliya *et al.* (Ref. 32) and Hiraka *et al.* (Ref. 28) (200 μeV FWHM).
[34] B. P. Burton, E. Cockayne, S. Tinte, and U. V. Waghmare, Phase Transitions **79**, 91 (2006).
[35] C. Stock, D. Ellis, I. P. Swainson, Guangyong Xu, H. Hiraka, Z. Zhong, H. Luo, X. Zhao, D. Viehland, R. J. Birgeneau, and G. Shirane, Phys. Rev. B **73**, 064107 (2006).
[36] G. Xu, P. M. Gehring, V. J. Ghosh, and G. Shirane, Acta Crystallogr., Sect. A: Found. Crystallogr. **60**, 598 (2004).
[37] A. Meyer, R. M. Dimeo, P. M. Gehring, and D. A. Neumann, Rev. Sci. Instrum. **74**, 2759 (2003).
[38] W. Chen and Z.-G. Ye (unpublished); Z.-G. Ye, P. Tissot, and H. Schmid, Mater. Res. Bull. **25**, 739 (1990).
[39] S. B. Vakhrushev (private communication).
[40] S. B. Vakhrushev, A. A. Naberezhnov, N. M. Okuneva, and B. N. Savenko, Phys. Solid State **37**, 1993 (1995).
[41] S. Vakhrushev, A. Ivanov, and J. Kulda, Phys. Chem. Chem. Phys. **7**, 2340 (2005).
[42] D. La-Orauttapong, J. Toulouse, Z. G. Ye, W. Chen, R. Erwin, and J. L. Roberston, Phys. Rev. B **67**, 134110 (2003).
[43] These authors show schematic diffuse scattering intensity contours in Fig. 4 of their paper (no data are shown) for PZN-4.5%PT and PZN-9%PT that are wrong because they do not possess the required crystal lattice symmetry.
[44] T. R. Welberry, D. J. Goossens, and M. J. Gutmann, Phys. Rev.

B **74**, 224108 (2006).
[45] T. R. Welberry, M. J. Gutmann, Hyungje Woo, D. J. Goossens, Guangyong Xu, and C. Stock, J. Appl. Crystallogr. **38**, 639 (2005).
[46] S. Wakimoto, G. A. Samara, R. K. Grubbs, E. L. Venturini, L. A. Boatner, G. Xu, G. Shirane, and S.-H. Lee, Phys. Rev. B **74**, 054101 (2006).
[47] M. Pasciak, M. Wolcyrz, and A. Pietraszko, Phys. Rev. B **76**, 014117 (2007).
[48] B. P. Burton and E. Cockayne, Phys. Rev. B **60**, R12542 (1999).
[49] V. V. Laguta, M. D. Glinchuk, S. N. Nokhrin, I. P. Bykov, R. Blinc, A. Gregorovic, and B. Zalar, Phys. Rev. B **67**, 104106 (2003).
[50] C. Boulesteix, F. Varnier, A. Llebaria, and E. Husson, J. Solid State Chem. **108**, 141 (1994).
[51] O. Svitelskiy, J. Toulouse, G. Yong, and Z.-G. Ye, Phys. Rev. B **68**, 104107 (2003).
[52] K. Hirota, Z.-G. Ye, S. Wakimoto, P. M. Gehring, and G. Shirane, Phys. Rev. B **65**, 104105 (2002).
[53] R. Comes, M. Lambert, and A. Guinier, Acta Crystallogr., Sect. A: Cryst. Phys., Diffr., Theor. Gen. Crystallogr. **26**, 244 (1970).
[54] S. N. Gvasaliya, B. Roessli, R. A. Cowley, P. Huber, and S. G. Lushnikov, J. Phys.: Condens. Matter **17**, 4343 (2005).
[55] S. Wakimoto, C. Stock, Z.-G. Ye, W. Chen, P. M. Gehring, and G. Shirane, Phys. Rev. B **66**, 224102 (2002).
[56] H. Sompolinsky and A. Zippelius, Phys. Rev. B **25**, 6860 (1982).
[57] P. M. Gehring, S.-E. Park, and G. Shirane, Phys. Rev. Lett. **84**, 5216 (2000).
[58] P. M. Gehring, S. B. Vakhrushev, and G. Shirane, in *Fundamental Physics of Ferroelectrics 2000: Aspen Center for Physics Winter Workshop*, AIP Conf. Proc. No. 535, edited by R. E. Cohen (AIP, New York, 2000), p. 314.
[59] P. M. Gehring, S. Wakimoto, Z.-G. Ye, and G. Shirane, Phys. Rev. Lett. **87**, 277601 (2001).
[60] P. M. Gehring, S.-E. Park, and G. Shirane, Phys. Rev. B **63**, 224109 (2001).
[61] V. Bovtun, S. Kamba, A. Pashkin, M. Savinov, P. Samoukhina, J. Petzelt, I. P. Bykov, and M. D. Glinchuk, Ferroelectrics **298**, 23 (2004).
[62] L. A. Shebanov, P. P. Kapostins, and J. A. Zvirgds, Ferroelectrics **56**, 53 (1984).
[63] H. Arndt and G. Schmidt, Ferroelectrics **79**, 149 (1988).
[64] B. Dkhil, J. M. Kiat, G. Calvarin, G. Baldinozzi, S. B. Vakhrushev, and E. Suard, Phys. Rev. B **65**, 024104 (2001).
[65] D. K. Agrawal, A. Halliyal, and J. Belsick, Mater. Res. Bull. **23**, 159 (1988).
[66] P. M. Gehring, W. Chen, Z.-G. Ye, and G. Shirane, J. Phys.: Condens. Matter **16**, 7113 (2004).
[67] H. W. King, M. Yildiz, S. H. Ferguson, D. F. Waechter, and S. E. Prasad, Ferroelectr., Lett. Sect. **31**, 55 (2004).
[68] P. Bonneau, P. Garnier, G. Calvarin, E. Husson, J. R. Gavarri, A. W. Hewat, and A. Morell, J. Solid State Chem. **91**, 350 (1991).
[69] Z.-G. Ye, Y. Bing, J. Gao, A. A. Bokov, P. Stephens, B. Noheda, and G. Shirane, Phys. Rev. B **67**, 104104 (2003).
[70] K. H. Conlon, H. Luo, D. Viehland, J. F. Li, T. Whan, J. H. Fox, C. Stock, and G. Shirane, Phys. Rev. B **70**, 172204 (2004).
[71] G. Xu, P. M. Gehring, C. Stock, and K. Conlon, Phase Transitions **79**, 135 (2006).
[72] G. Xu, D. Viehland, J. F. Li, P. M. Gehring, and G. Shirane, Phys. Rev. B **68**, 212410 (2003).
[73] J.-H. Ko, S. Kojima, A. A. Bokov, and Z.-G. Ye, Appl. Phys. Lett. **91**, 252909 (2007).
[74] G. Xu, J. Wen, C. Stock, and P. M. Gehring, Nature Mater. **7**, 562 (2008).
[75] D. Viehland, S. J. Jang, L. E. Cross, and M. Wuttig, Phys. Rev. B **46**, 8003 (1992).
[76] I. G. Siny and T. A. Smirnova, Ferroelectrics **90**, 191 (1989).
[77] S. B. Vakhrushev and N. M. Okuneva, in *Fundamental Physics of Ferroelectrics*, AIP Conf. Proc. No. 626, edited by R. E. Cohen (AIP, New York, 2002), p. 117.
[78] http://arxiv.org/ftp/cond-mat/papers/0506/0506132.pdf
[79] T. Egami, W. Dmowski, I.-K. Jeong, R. H. Heffner, J.-S. Park, K.-S. Hong, M. Hehlen, and F. Trouw, in *Fundamental Physics of Ferroelectrics*, Williamsburg Conf. Proc., edited by R. E. Cohen and P. M. Gehring (Washington, D.C., 2004), p. 58. (http://people.gl.ciw.edu/cohen/meetings/ferro2004/Ferro2004Abstractbook.pdf).
[80] W. Dmowski, S. B. Vakhrushev, I.-K. Jeong, M. P. Hehlen, F. Trouw, and T. Egami, Phys. Rev. Lett. **100**, 137602 (2008).
[81] M. Roth, E. Mojaev, E. Dul'kin, P. Gemeiner, and B. Dkhil, Phys. Rev. Lett. **98**, 265701 (2007).
[82] J. Toulouse, Ferroelectrics **369**, 203 (2008).
[83] C. Stock, R. J. Birgeneau, S. Wakimoto, J. S. Gardner, W. Chen, Z.-G. Ye, and G. Shirane, Phys. Rev. B **69**, 094104 (2004).
[84] G. Xu, Z. Zhong, Y. Bing, Z.-G. Ye, C. Stock, and G. Shirane, Phys. Rev. B **67**, 104102 (2003).
[85] A. Aharony (private communication).
[86] V. Westphal, W. Kleemann, and M. D. Glinchuk, Phys. Rev. Lett. **68**, 847 (1992).
[87] R. Pirc and R. Blinc, Phys. Rev. B **60**, 13470 (1999).
[88] R. Fisch, Phys. Rev. B **67**, 094110 (2003).